Crashworthiness Analysis with Enhanced Composite Material Models in LS-DYNA – Merits and Limits

K. Schweizerhof*†, K. Weimar†, Th. Münz†, Th. Rottner*

* Institute for Mechanics, University of Karlsruhe, D-76128 Karlsruhe
† CAD-FEM GmbH, Marktplatz 2, D-85567 Grafing

key words: composites, crash, shells, damage

Crashworthiness Analysis with Enhanced Composite Material Models in LS-DYNA – Merits and Limits

K. Schweizerhof, K. Weimar, Th. Münz, Th. Rottner

Abstract

The composite materials in LS-DYNA have been enhanced to improve the capabilities for crashworthiness simulations of shell type structures. In particular several damage type models have been considered and modified. The improved models have been tested and finally critically reviewed. A closer look at the complexity of the crushing behaviour of composite shell structures in the case of large deformations reveals the merits and the limits of any continuum material model for general applications.

1 Introduction

The composite material models in LS-DYNA have been reviewed and enhanced to improve the capabilities for crashworthiness simulation and also to provide — if possible — a general analysis tool for shell like structures made from composite, often layered material. Thus first the composite damage model material 54 in LS-DYNA based on failure surfaces and rather heuristic damage measures is discussed and enhanced. Then a consistent damage theory based model with a smooth damage evolution as originally proposed in [9] is presented and discussed. Both models are enhanced by strain based failure criteria (≡ element elimination). Finally some simple element tests are performed and the limits of continuum models to simulate shell structures made from composite materials in crashworthiness analyses are discussed.

Due to limited space, the presentation is limited to an overview and the theoretical background is only briefly discussed.

2 Material 54 – material model and failure parameters

This composite damage material allows to describe anisotropic, linear elastic behaviour if the material is undamaged, which is valid for many composites. The various damage criteria introduce then a nonlinearity into the material model. Different stress- or strain related failure criteria have been implemented and enhanced within the CRASURV project [13]. To model some pre-damaging processes, known from experiments, additional parameters can be set on the choice of the analyst. They are discussed in more detail below in the context of structural computations.

2.1 Input data and Failure Criteria

The material input data consist of material properties like Youngs modulus, Poisson ratio and shear modulus in the various directions, see table 1, the direction of anisotropy as well as of strengths in fiber or matrix direction, see table 2. The strengths in fiber and

E_x, E_y, E_z	Youngs modulus
ν_{xy}, ν_{yz}, ν_{xz}	Poisson ratio
G_{xy}, G_{yz}, G_{xz}	Shear modulus

Table 1: Elastic material properties of LS-DYNA Material 54

X_t	longitudinal tensile strength
X_c	longitudinal compressive strength
Y_t	transverse tensile strength
Y_c	transverse compressive strength
S_c	shear strength

Table 2: Strengths in fiber and matrix direction of LS-DYNA Material 54

matrix direction are different for tension and compression. In the following equations the failure criteria are given:

Tensile fiber mode (Fiber rupture) $\sigma_{11} \geq 0$:

$$e_f^2 = \left(\frac{\sigma_{11}}{X_t}\right)^2 - 1 \begin{cases} \geq 0 \text{ failed} \\ < 0 \text{ elastic} \end{cases} \tag{1}$$

Compressive fiber mode (Fiber buckling and kinking) $\sigma_{11} < 0$:

$$e_c^2 = \left(\frac{\sigma_{11}}{X_c}\right)^2 - 1 \begin{cases} \geq 0 \text{ failed} \\ < 0 \text{ elastic} \end{cases} \tag{2}$$

Tensile matrix mode (Matrix cracking under transverse tension and shearing):

$$e_m^2 = \left(\frac{\sigma_{22}}{Y_t}\right)^2 + \left(\frac{\tau}{S_c}\right)^2 - 1 \begin{cases} \geq 0 \text{ failed} \\ < 0 \text{ elastic} \end{cases} \tag{3}$$

Compressive matrix mode (Matrix cracking under transverse compression + shearing):

$$e_d^2 = \left(\frac{\sigma_{22}}{2S_c}\right)^2 + \frac{\sigma_{22}}{Y_c}\left[\frac{Y_c^2}{4S_c^2} - 1\right] + \left(\frac{\tau}{S_c}\right)^2 - 1 \begin{cases} \geq 0 \text{ failed} \\ < 0 \text{ elastic} \end{cases} \tag{4}$$

These criteria are stress-related, whereas it is sometimes desirable to limit also the strains. In material model 54 this is possible using the parameters `DFAILT`, `DFAILC`, `DFAILM`, `DFAILS` and `EFFSTRN`, see table 3.

After some compressive failure of the matrix, the tensile and compressive strength of the composite material can be reduced, which can be modeled for brittle materials with the parameters `FBRT` and `YCFAC`, see table 4. Due to large compressive deformations and thus reduced element size resulting in small time steps, elements can also fail, if their time step decreases below a certain value given in `TFAIL`, which is to some extent related to the `EFFSTRN` parameter which has no favourite direction. Another heuristic parameter, also given in table 4 is `SOFT`, which allows to reduce Youngs moduli and

DFAILT	maximum strain for fiber tension
DFAILC	maximum strain for fiber compression
DFAILM	maximum strain for matrix (tension and compression)
DFAILS	maximum shear strain
EFFSTRN	effective strain

Table 3: Strain limiting parameters of LS-DYNA Material 54

FBRT	reduction factor for tensile fiber strength after matrix failure
YCFAC	reduction factor for compressive fiber strength after matrix failure
TFAIL	time step failure
SOFT	softening factor for elements in crashfront

Table 4: Additional softening/failure parameters

strengths of elements neighboured to failed elements. With this, a crushing process with a damage front can be simulated, because in experiments a damage of material parts, which are not yet undergoing large deformations, is observed. Using a trigger, a controlled crash process can be initiated then; the elements will first fail at the trigger and then because of the pre-damaged material a stable so called crashfront will occur, as it is observed in experiments. For a more detailed description of the other material parameters we refer to the LS-DYNA reference manuals [3] [4].

2.2 One element test examples

For a better understanding of the introduced parameters some computations with an one element test problem are performed, see figure 1. Here, only one layer through the thickness is used for simplicity and clarity.

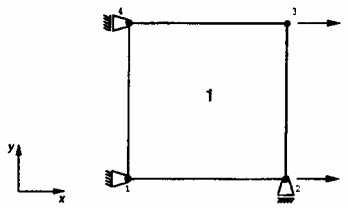

Figure 1: One element test problem

The orthotropic material data are: $E_x = 45847.0N/m^2$, $E_y = 17506.0N/m^2$ and $E_z = 17506.0N/m^2$ and $\nu_x = \nu_y = 0.1$, $\nu_z = 0.331$. The chosen limit strengths are: In fiber direction $X_t = 1120\ N/mm^2$, $X_c = 900\ N/mm^2$; in matrix direction $Y_t = 39\ N/mm^2$, $Y_c = 134\ N/mm^2$ and in shear $S_c = 77\ N/mm^2$.

2.3 Tension and compression in fiber direction

First, a loading in fiber direction (as is shown in figure 1) is applied to the element.

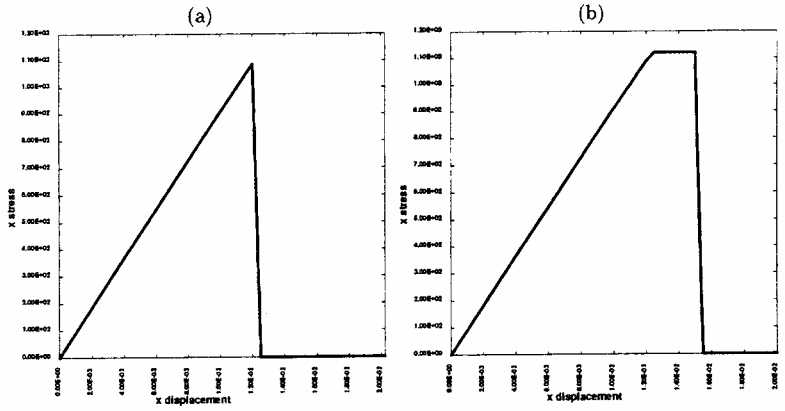

Figure 2: Stress-displacement curve (a) `DFAILT = 0.0`, (b) `DFAILT = 0.3`

As can be seen in diagram 2(a), the element stress in fiber direction increases, until it reaches the maximum value of 1120 N/mm^2. Then the fibers are breaking, the stress in fiber direction is reduced to zero. In addition all other stresses in the element are set to zero. The material behaviour is linear-brittle.

The curve in figure 2(b) shows the same loading but with the parameter `DFAILT` set to 0.03, the element fails at a tensile strain of 3%. After reaching the maximum stress in fiber direction, the stress remains constant until the maximum strain is reached. Thus by using the strain limiting parameters as failure criteria the material behaviour is elasto-plastic up to failure.

2.4 Combined tension and compression in fiber and matrix direction

Now the element is loaded in matrix direction. For the failure in this direction, the strengths Y_t and Y_c are responsible. As strain criterion `EFFSTRN` could be used, if a separate strain failure criterion for the matrix direction is not set.

In general, the same behaviour as in fiber direction can be observed. The difference in the strain values in y direction visible in smaller displacements at failure is caused by the fact, that the effective strains also include the strains in the other directions and thus are not exactly identical to the matrix directional strains.

As mentioned in section 2.1, the strengths may be reduced after the matrix compressive failure. In order to achieve this, the parameters `FBRT` and `YCFAC` can be used. With the `FBRT` parameter the fiber tensile strength after matrix failure can be reduced to $X_t^* = X_t$*`FBRT`. If the new limit strength X_t^* is lower than the actual stress, then X_t^* is taken as tensile stress, when combined with the strain failure criterion. In the current example, the parameter `FBRT` is set to 0.5, so that the fiber tensile strength after matrix compressive failure is $X_t^* = 560\ N/mm^2$ as depicted in figure 3(a). The same can be done for the fiber compressive strength after matrix compressive failure with the parameter `YCFAC`. The new fiber compressive strength after matrix compressive failure

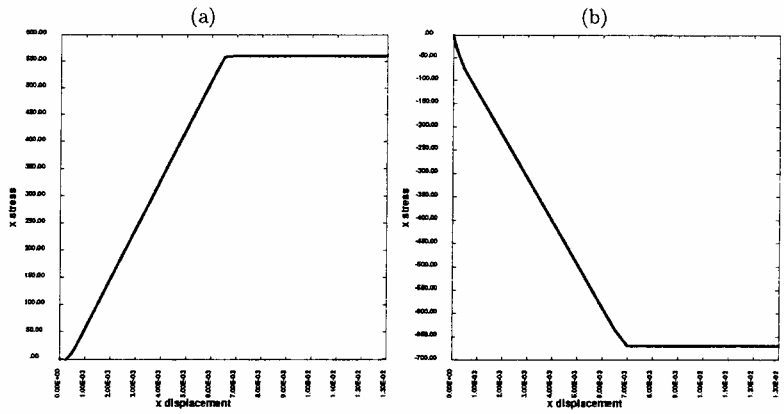

Figure 3: Stress displacement curve after matrix compression failure – (a) tension, fiber direction (FBRT = 0.5), (b) compression, fiber direction (YCFAC = 5.0)

becomes $X_c^* = Y_c$*YCFAC. In the test example, YCFAC is chosen to 5.0, X_c^* is then 670 N/mm^2 after matrix compressive failure, as is shown in figure 3(b). It is clear, that X_c^* must be smaller than X_c.

2.5 Computations with multilayered materials

The former simulations were performed using only one layer, which is possible for every composite material, because lay-ups can also be considered in a macroscopic manner. In many practical applications the material properties are measured using not only one layer but the whole lay-up. As a result, the anisotropic material constants of the lay-up are obtained. Nevertheless it may be useful to simulate the composite structure using different layers through the thickness. Then the failure criteria are valid for each layer separately.

It is certainly a subject of further studies to discuss the correct simulation of a multi-layered composite. Using a smeared type model, failure is more likely to be brittle, thus failure is obtained, when the criteria are fulfilled in one integration point throughout the thickness. Using the multi-layer approach the so-called ply-count method is appropriate. Both approaches can be chosen in LS-DYNA.

Some results of the simulations mentioned above can be visualized also for layered composite material, focusing on the fiber/matrix tensile/compressive modes, that can be observed using the LS-TAURUS fringe plot capability with fringes 81 (tensile fiber mode), 82 (compressive fiber mode), 83 (tensile matrix mode) and 84 (compressive matrix mode).

Remark: Material model 54 allows for wide spread of a rather heuristic setting of the failure parameters resp. damage parameters. Thus fairly good adjustments to particular experiments are possible. However, the analyst has to keep in mind, that single ply failures in lay-ups are hardly possible without affecting the neighbouring layers directly and immediately. Thus it would be desirable to have more information from experi-

ments, in particular, about strengths in the post-failure regime. Finally the range of applications should be limited to the regime, where material data are obtainable from tests. This certainly limits the analysis of large deformation problems with composites in the compressive regime.

3 Material 58a – material model and failure parameters

A first step of the material model 58 in LS-DYNA is described in [9]. The material law – recently again implemented as material 58a – is formulated for plane stress conditions which is then assumed to be the state of stress in a shell. Thus the material application is restricted to plate and shell type problems. In a standard layer-wise approach the plane stress assumption is also taken for each layer of a laminate.

Material model 58a is a so-called elastic damage model, where it is assumed that the deformation introduces microcracks and cavities into the material. These defects cause primarily stiffness degradation with rather small permanent deformations unless the material undergoes rather high loading and is not close to deterioration. Based on the suggestions of Hashin four failure criteria are considered to be valid for each lamina of a composite structure [9] (see also figure 4):

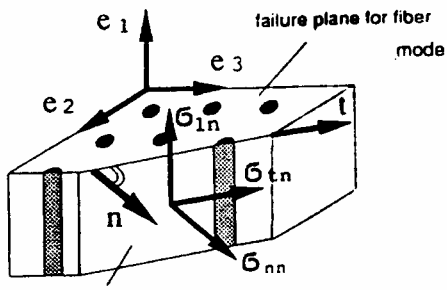

Figure 4: Failure planes of the lamina

Tensile fiber mode (Fiber rupture) $\sigma_{11} \geq 0$:

$$e_m^2 = \left(\frac{\sigma_{11}}{X_t}\right)^2 - 1 \begin{cases} \geq 0 \text{ failed} \\ < 0 \text{ elastic} \end{cases}$$

Compressive fiber mode (Fiber buckling and kinking) $\sigma_{11} < 0$:

$$e_c^2 = \left(\frac{\sigma_{11}}{X_c}\right)^2 - 1 \begin{cases} \geq 0 \text{ failed} \\ < 0 \text{ elastic} \end{cases}$$

Tensile matrix mode (Matrix cracking under transverse tension and shearing) $\sigma_{22} \geq 0$:

$$e_m^2 = \left(\frac{\sigma_{22}}{Y_t}\right)^2 + \left(\frac{\tau}{S_c}\right)^2 - 1 \begin{cases} \geq 0 \text{ failed} \\ < 0 \text{ elastic} \end{cases}$$

Compressive matrix mode (Matrix cracking under transverse compression and shearing) $\sigma_{22} < 0$:

$$e_d^2 = \left(\frac{\sigma_{22}}{Y_c}\right)^2 + \left(\frac{\tau}{S_c}\right)^2 - 1 \begin{cases} \geq 0 \text{ failed} \\ < 0 \text{ elastic} \end{cases}$$

The failure criteria – the above valid for unidirectionally reinforced composites – have to be interpreted as so-called loading criteria and play the role of threshold variables in the damage model. As only the undamaged part of of a cross section can carry load, the stresses in the criteria above should be interpreted as effective stresses $\hat{\sigma_{ij}}$ referred to the net area. The following simple relationship between effective stresses $\hat{\sigma}$ and nominal (true) stresses σ hold:

$$\hat{\sigma} = \begin{bmatrix} \hat{\sigma}_{11} \\ \hat{\sigma}_{22} \\ \hat{\sigma}_{12} \end{bmatrix} = \begin{bmatrix} \frac{1}{1-\omega_{11}} & 0 & 0 \\ 0 & \frac{1}{1-\omega_{22}} & 0 \\ 0 & 0 & \frac{1}{1-\omega_{12}} \end{bmatrix} \begin{bmatrix} \sigma_{11} \\ \sigma_{22} \\ \sigma_{12} \end{bmatrix}.$$

It must be noted, that the two damage parameters ω_{11} and ω_{22} assume different values for tension (ω_{11t} and ω_{22t}) and compression (ω_{11c} and ω_{22c}) in order to account for the phenomenon of one-sidedness which is typical for many materials. In contrast to ω_{11} and ω_{22} the damage parameter for shear ω_{12} is independent of the sign of the shear stress τ. As a consequence the constitutive tensor $\mathbf{C}$ is a function of the damage parameter:

$$\mathbf{C}(\omega) = \frac{1}{D} \cdot \begin{pmatrix} (1-\omega_{11})E_{\|} & (1-\omega_{11})(1-\omega_{22})\nu_{21}E_{\perp} & 0 \\ (1-\omega_{11})(1-\omega_{22})\nu_{12}E_{\|} & (1-\omega_{22})E_{\perp} & 0 \\ 0 & 0 & D(1-\omega_{12})G \end{pmatrix}$$

with

$$D = 1 - (1-\omega_{11})(1-\omega_{22})\nu_{12}\nu_{21} > 0.$$

The state of damage is unchanged in the elastic range, which is bounded by the loading surfaces resp. the threshold values described by the failure criteria. The stress components in the failure criteria are replaced by the effective stresses $\hat{\sigma}$ and become:

$$\begin{aligned} f_{\|} &= \frac{\sigma_{11}^2}{(1-\omega_{11c,t})^2 X_{c,t}^2} - r_{\|c,t} = 0 \\ f_{\perp} &= \frac{\sigma_{22}^2}{(1-\omega_{22c,t})^2 Y_{c,t}^2} + \frac{\tau^2}{(1-\omega_{12})^2 S_c^2} - r_{\perp c,t} = 0. \end{aligned}$$

The strength quantities $X_{c,t}$, $Y_{c,t}$ and the damage parameters $\omega_{11c,t}$, $\omega_{22c,t}$ for compression resp. tension are:

$$X_{c,t} = \begin{cases} X_t & \text{if } \sigma_{11} \geq 0 \\ X_c & \text{if } \sigma_{11} < 0 \end{cases}$$

and

$$Y_{c,t} = \begin{cases} Y_t & \text{if } \sigma_{22} \geq 0 \\ Y_c & \text{if } \sigma_{22} < 0 \end{cases}.$$

For the shear damage parameter ω_{12} respectively the shear strength S_c no difference is made for loading in either direction. The loading criteria are depicted in figure 5 in the space of effective stresses. It is clearly visible that the general failure surface is made up from various different surfaces.

The state of damage is assumed to change once the state of stress is outside of the failure criteria. For a detailed description it is referred to [9]. For the damage evolution – the

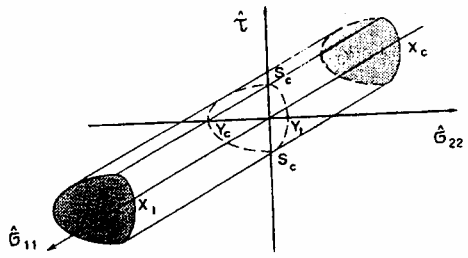

Figure 5: Multisurface loading criteria, formed by $f_{\|}$ and $f_{\perp}$ in the space of effective stresses

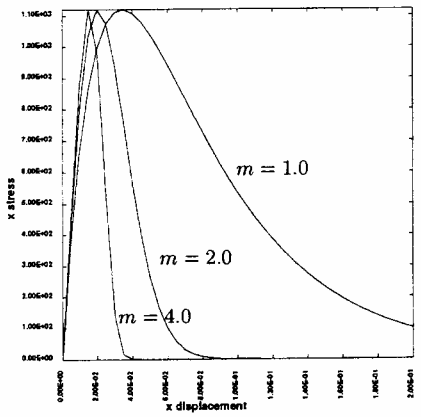

Figure 6: Stress-displacement curve for $m = 1.0$, 2.0 and 4.0

change of the damage parameters – many evolution laws are possible. The assumed relation in material 58a is

$$\omega_i = 1 - \exp[-\frac{1}{m_i e}(\frac{\varepsilon_i}{\varepsilon_f})^{m_i}] \qquad \begin{array}{l}\varepsilon_f \text{ is the nominal failure strain} \\ \varepsilon_{f\|} = \frac{X_{t,c}}{E_{\|}};\ \varepsilon_{f\perp} = \frac{Y_{t,c}}{E_{\perp}}\end{array}$$

The main difference to material model 54 lies in the smooth increase of damage; no sudden change of material behaviour occurs which appears to be physically more correct. The damaging progress starts with the deformation of the elements. The parameters m_i describe the development of the different failure modes like tension, compression and shear in the various directions depending on the strains. Then a damage parameter ω_i is computed for each direction and a stress-strain relation can be obtained. $\omega_i = 1.0$ denotes complete damage. In figure 6 the normalized stress-displacement diagram for different values of m is shown (see also [9]) for the uniaxial case.

3.1 Limits of Material 58a – uniaxially based

The material model as described in [9] is initially based on UD reinforced composite and therefore has a complete decoupling of the 11-failure mode from shear failure. Thus the failure criteria overestimate the strength of a lamina in 11-direction, if shear is present, resp. underestimate the strength in 22-direction when shear loading is superimposed to a uniaxial loading in 22-direction. Thus the validity for the simulation of fabrics with equal strength in 11- and 22-directions seems to be limited. How well fabrics can be simulated is dependent on the calibration of the material model and the loading. In addition, the adjustment of the stress-strain curves using the m-values is rather tedious.

Localization

If the same problem as in figure 1 is considered, but now discretized with 4 elements of equal size, localization can be obtained as follows. After the elements reach their maximal stress values, strain softening starts and due to minor numerical differences some elements are further deformed, whereas other elements are unloaded. Such effects known as localization have to be expected with the strain softening damage model and introduce considerable mesh size dependencies into any FE computation. These mesh dependencies have to be considered in each analysis and make any simulation of unknown problems questionable unless some adjustment with known results can be made. A better suggestion would be to introduce a correct analysis of the localization zones which is beyond the scope of this study.

3.2 Material 58a – Modification of the strain softening part

To avoid the observed localization effects in many cases in an "engineering" type approach a simple modification is introduced. The idea is to modify the damage evolution law such that the stress does not fall below a threshold value, the limit stress ("yield-stress"). After reaching this yield-stress the evolution law for the damage parameter ω is modified to

$$\omega = 1 - \frac{\alpha \cdot X_{t,c}}{E \cdot \varepsilon}$$

in the uniaxial case. A new parameter α with $0 \leq \alpha \leq 1$ is introduced to characterize this yield-stress to have some relation to the strength value. The original and the modified evolution of the damage parameter ω is depicted for $m = 1.0$ in figure 7(left); the resulting stress-strain diagram is shown in figure 7(right) (the parameter α is identical to `fac`). In figure 7(right) it is visible, that the element stress remains constant at $\alpha * X_{t,c}$ after passing the limit value $X_{c,t}$.

However, we have to note that with a factor $\alpha < 1$ localization is still present; damage growth is only in the first affected elements. Without softening ($\alpha = 1.0$) however, the strains grow in all elements in a similar fashion.

In addition to this damage modification the material model was also enhanced to allow element resp. layer failure with maximum effective strain. Also the crashfront model was added to allow a combination with all the other desired features already described for material model 54.

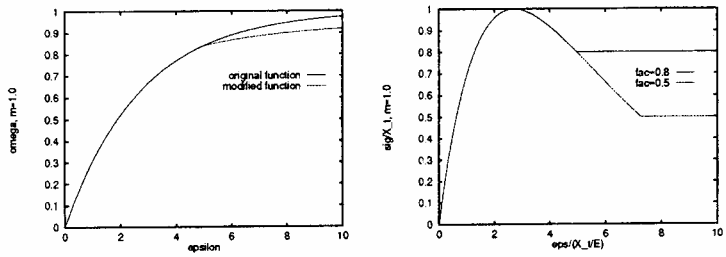

Figure 7: Original and modified damage parameter for $m = 1.0$ and stress-strain diagram for $\alpha = 0.5$ and 0.8

3.3 Calibration

Calibration of the material data is performed using simple tensile tests. This is straightforward for the 11- and 22-directions. Simply the strength and the according strain values have to be chosen from a measured stress-strain curve.

The softening part of the stress-strain curve is anyhow rather undetermined and is almost impossible to measure. Thus it may also be advisable to reduce the strength completely to zero, when the stresses reach the loading surface in particular for tension. This can be accomplished by setting the failure strain for element elimination resp. lamina elimination to this value e.g. $\varepsilon_{t,fail} = dfailt$ resp. for the other directions of the anisotropic composite material.

3.4 Simple approximation of the stress-strain curve

As from material testing usually stress-strain curves are known, it seems a better way — at least from the user point of view — to use these curves directly for a fit of the material data. The curves, for which the proposed fit is valid, have the following form for unidirectional loading, see figure 8. Then the values σ_f and ε_q can be used to determine

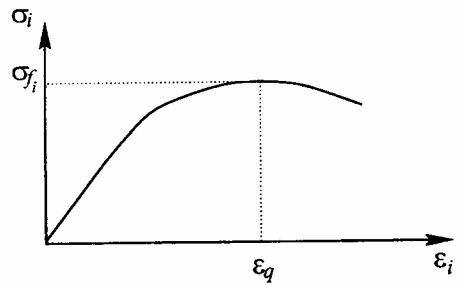

Figure 8: Assumed stress-strain curve for brittle composite materials

the nonlinear relationship:

$$\sigma_i = \exp[-\frac{-\ln\beta_i}{e}(\frac{E_i\varepsilon_i}{\sigma_{fi}})^{\frac{1}{\ln\beta_i}}]\frac{\varepsilon_i}{E_i} \qquad \text{with } \beta_i = \frac{\varepsilon_q}{\sigma_{fi}} \cdot E_i; \qquad \text{only } \beta > 0 \text{ allowed!} \quad (5)$$

The evolution of the damage parameter is modified accordingly. For each of the five damage parameters ω_{11t}, ω_{11c}, ω_{22t}, ω_{11c} and ω_{12} and the corresponding stress-strain curves a fit can be achieved. σ_{fi} is assumed to be identical to $X_{c,t}$; $Y_{c,t}$, S_c respectively.

3.5 Modification of failure criteria for the simulation of fabrics

The material model as originally described in [9] is limited to materials with a failure surface which is made up from different failure criteria for each direction. Fabrics, however, fail almost identically in the 11 and 22 directions. Thus two different material models following the damage approach as developed in [9] have been implemented in LS-DYNA.

All additional failure criteria as described for material 58a also apply for materials 58b and 58c.

3.5.1 Smooth failure surfaces – material 58b

For the smooth failure surface model – denoted as material 58b – the failure criterion in the 11-direction is taken to be identical to the failure criterion in the 22-direction.

$$f_{11} = \frac{\sigma_{11}^2}{(1-\omega_{11c,t})^2 X_{c,t}^2} + \frac{\tau^2}{(1-\omega_{12})^2 S_c^2} - r_{\|c,t} = 0$$

The other failure criterion remains unmodified.

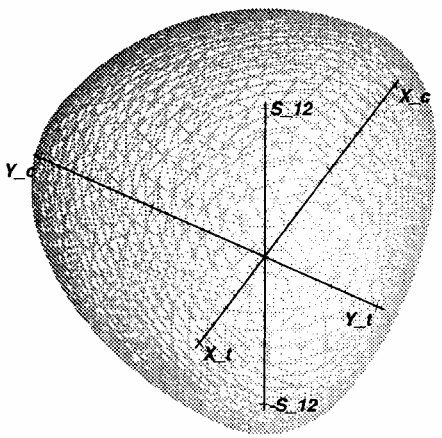

Figure 9: Smooth failure surfaces used as loading criteria for damage material model 58b

Thus, the multi-surface loading criterion in the space of effective stresses looks as depicted in figure 9. Each surface is checked independently. For the evolution of the shear damage value ω_{12} always the larger value resulting from either loading criterion 11 or 22 is taken. By using the same strength values in both directions

$$\begin{aligned} Y_c &= X_c \quad \text{further compressive strength} \\ Y_t &= X_t \quad \text{further tensile strength} \end{aligned}$$

a fabric type damage behaviour can be achieved.

In combination with the modification for the strain softening part as described in section 3.2 some adjustments can be made for the post-failure part in the larger strain regime though the validation of such an assumption is rather limited.

3.5.2 Non-smooth failure surfaces – material 58c

In order to allow an almost uncoupled failure of an arbitrary composite, all failure criteria are taken to be independent of each other.

$$\begin{aligned} f_{\parallel} &= \frac{\sigma_{11}^2}{(1-\omega_{11c,t})^2 X_{c,t}^2} - r_{\parallel c,t} = 0 \\ f_{\perp} &= \frac{\sigma_{22}^2}{(1-\omega_{22c,t})^2 Y_{c,t}^2} - r_{\perp c,t} = 0 \\ f_s &= \frac{\tau^2}{(1-\omega_{12})^2 S_c^2} - r_s = 0 \end{aligned}$$

Thus the multi-surface criterion in the space of effective stresses looks as depicted in figure 10.

This criterion allows to treat all stress resp. material components in an uncoupled fashion as the damage evolution is concerned. The complete stress-strain state is still described by the elastic "damaged" constitutive relations and contains a coupling.

3.5.3 Nonlinear Stress-Strain curve for Shear

Experiments with fabrics under a loading which is not in fiber direction [6] show a considerably nonlinear load deflection curve, which is almost bilinear, whereas the loading in fiber direction leads to rather linear behaviour. Thus a special nonlinear damage evolution law is introduced for the shear part of material 58c. The input is via a nonlinear stress strain curve which is defined by two pairs of stress-strain values, see figure 15. The first pair is τ_1, γ_1 and a nonlinear curve identical to the one defined by equation (5) is assumed between the origin and τ_1, γ_1. The second pair S_c, γ_{MS} defines the end of a linear curve part from (τ_1/γ_1). The second pair can be viewed as failure stress resp. failure strain and the layer is then assumed as failed if these values are reached. Thus as a default a rather brittle failure is assumed. If a more elasto-plastic type behaviour has to be modeled an additional stress limiter $SLIMS$ can be introduced, which allows to keep the stress constant beyond the shear strain γ_{MS} setting the value of $SLIMS$ to one. If the value is set to a value smaller than one then the stress limit is assumed to be $SLIMS * S_c$ and no failure is assumed for a shear strain of γ_{MS}. It has to be noted that the stress limit must be greater than τ_1 and that $SLIMS \leq 1.0$.

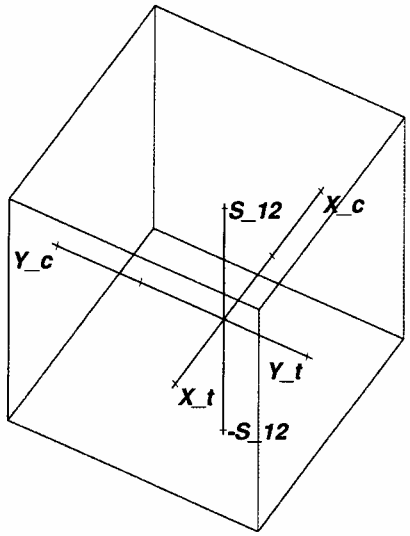

Figure 10: Non-smooth failure surfaces used as loading surface for damage material model 58c

3.6 Calibration

Calibration for the new models is achieved for the 11- and 22-directions in tension and compression, as it is done for material 58a. The shear component can be adjusted by a 45° tension resp. compression test, however then in material 58b also the failure criteria resp. loading criteria for the 11 and 22 direction are involved. As is well known, a torsion test would allow for a completely independent adjustment, but this is not performed in most cases for the investigation of composite type structures.

It is also not quite clear, if the nonlinear shear-strain curve introduced allows to capture

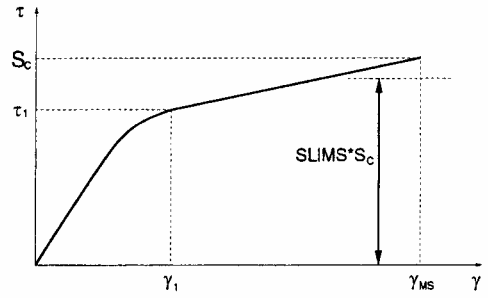

Figure 11: Stress-strain diagram for shear

all nonlinear effects for the behaviour of fabrics under arbitrary loading.

4 45° tension test

If the membrane loading is in 0° or 90° direction, thus in fiber or matrix direction, neither bending nor shear failure are important in most cases and as a consequence the main aspect in the simulations is to determine failure parameters in compressive direction; the other parameters are then almost decoupled. Obviously it is much more difficult, if this is not the case. For example, for a simple tension test under 45° tensile and shear failure are coupled. With the LS-DYNA material 54 this can not be modeled, unless the strains are limited by DFAILC. With the modified damage model, material 58a, 58b and 58c, curves for a more nonlinear behaviour (with regard to the curvature) in the stress strain curves are possible.

In [6] some tension tests are preformed for different materials; here the data for CARBON G 803/M10 are used. In figure 3-4 in [6] the tension test results for the 0° tension test can be found.

For the finite element simulations of the tensile test, the system shown in figure 1 is used.

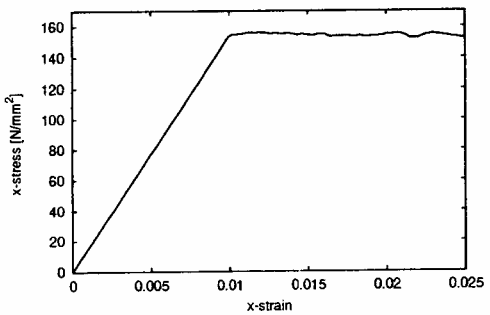

Figure 12: Carbon 0°/90°, 45° tension test, material 54

Choosing material 54, the 0° tension test can easily be simulated as it is almost linear up to failure. The measured curve of the 45° tension test, however, shows a slightly nonlinear, almost bilinear behaviour. For the shear strains the first part is slightly nonlinear up to a strain of about 0.9% and a stress of 90 MPa and the second part is linear up to a strain of about 3.8% and stresses increasing up to 156 MPa. In the simulation with material 54, see figure 12 after the shear failure in the Chang-Hashin criterion, the element stresses remain constant and do not increase any more. The behaviour is linear in the first part dominated by the initial moduli, thus the limit stresses are reached by a fairly small strain. The real nonlinear response cannot be simulated.

Using material 58 with damage, the situation is quite different. The 0° tension test can also be simulated without difficulties, the parameters $m_{f,t}$ (fiber, tension) can be easily adjusted, e.g. by setting the proper strain $\varepsilon_{q(f,t)}$ (see equation (5)).

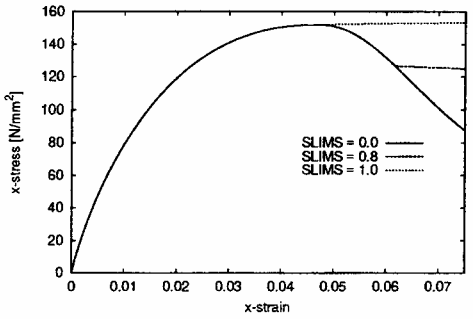

Figure 13: Carbon 0°/90°, 45° tension test, material 58a

For the simulation for the 45° tensile test, various additional parameters can be chosen, as m_s resp. the proper shear strain $\varepsilon_{q(s)}$, see equation (5), in combination with the softening parameter introduced in section 3.2. The parameter $m_{f,t}$ resp. $\varepsilon_{q(f,t)}$ remains unchanged, because the 0° tension test must also be fulfilled. In figure 13 the curves for different limit stresses are depicted; The stresses in x-direction are just about twice as large as the shear strains given in the input taken from the measurements. It can also be seen, that with softening as originally introduced in [9] the stresses decrease to zero after the maximum value was reached. With the parameter $SLIMS$ set to 0.8, the stress can be kept constant after softening. With $SLIMS = 1.0$ there is no decrease after shear failure. Varying the value of m_s resp. $\varepsilon_{q(s)}$, the stress-strain curve can be better adjusted to the measured curve in [6]. The bilinear behaviour cannot be achieved, but the results are significantly better than using the LS-DYNA Material 54 with which a hardening type of failure can not be modeled.

The analysis with material 58b shows – see figure 14 – that as in material 58a the shear failure dominates in both criteria; as the compressive and tensile strength are much higher, they do not affect the behaviour significantly in this deformation range and the curve shows only very little deviation from the curves obtained with material 58a.

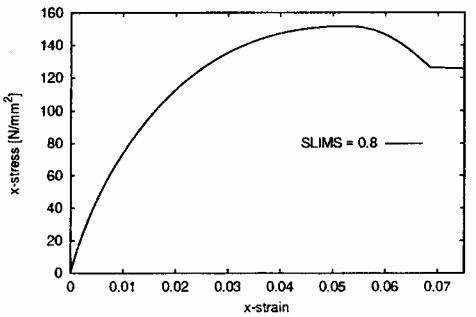

Figure 14: Carbon 0°/90°, 45° tension test, material 58b

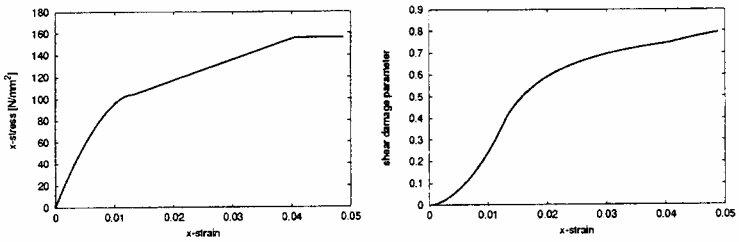

Figure 15: Stress-strain and shear damage parameter diagram

Nonlinear stress strain curve for shear

The new material model 58c allows to model fabrics with independent damage also in shear. In particular, a nonlinear stress strain curve for shear can be used. The 45° tension test using the corresponding curve from [6] shows the result given in figure 15(left) for the stress strain curve as mentioned above. This result has to be compared with the curves in figure 13 and 14 setting $SLIMS = 1.0$. Obviously the stress in x-direction is about twice the shear stress in 12-direction. The nonlinear dependency of the shear stress is quite visible in the x-stress curve. This is also due to the effect that the shear stress behaviour is dominating, as the 11- and 22 directions remain almost undamaged. The difference in the maximum stress and the corresponding strains are then rather small compared to a material without damage in 11- and 22-direction. The shear-damage parameter evolution is shown in figure 15(right).

The implementation of the nonlinear stress strain curve for shear allows also the use in combination with material 58a and 58b. However, calibration becomes rather difficult then.

5 Elasto-plastic models

The description is included for reasons of completeness only.

5.1 Faceted failure surface (Material 59a)

This is an elastic-plastic material, where the strength values in each orthotropy direction, as well as the shear strength are taken for the yield function. This results in a faceted surface envelope, which is valid for shell elements only. The failure surfaces are:

$$\sigma_{1t} = \alpha X_T \tag{6}$$

$$\sigma_{1c} = -X_c \tag{7}$$

$$\sigma_{2c} = \alpha Y_t \tag{8}$$

$$\sigma_{2c} = -Y_c \tag{9}$$

$$\sigma_{12} = \sigma_{23} = \sigma_{13} = \pm S_c. \tag{10}$$

This is very similar to the non-smooth failure surface depicted in figure 10. It must be noted that transverse shear is also considered in material 59a. Setting α to a certain

value allows to limit the tensile part of the failure surface after the first tensile failure. If $\alpha = 1$ is chosen, this results in a fully elastic-plastic model with the initial strength values for the failure surface. $\alpha = 0$ sets all tensile strengths to zero after failure, thus only compressive loads and shear can be carried after the corresponding failure.

5.2 Ellipsoidal failure surface (Material 59b)

This is an elasto-plastic material, for which the strength values are taken to form an ellipsoidal surface with the axes parallel to the axes of orthotropy.

The failure surface is then:

$$f = \frac{4[\sigma_1 - \frac{X_t - X_c}{2}]^2}{(X_t + X_c)^2} + \frac{4[\sigma_2 - \frac{Y_t - Y_c}{2}]^2}{(Y_t + Y_c)^2} + \frac{\sigma_{12}^2}{S_c^2} + \frac{\sigma_{13}^2}{S_c^2} + \frac{\sigma_{23}^2}{S_c^2} - 1 \qquad (11)$$

This surface is similar but not identical with the Tsai-Wu criterion. In particular it does not contain a coupling term between the orthotropy directions. It seems to be a model working well for materials with strength values not differing too much.

5.3 Crash front

Both models described above (Materials 59a and 59b) can be combined with the crash-front model.

5.4 Other failure criteria in material 59a and 59b

Failure in tension and failure with time stepsize limits – both based on limiting strains – as well as a limiting effective strain have been implemented. Thus, the element fails with large tensile strains resp. large compressive strains or large effective strains and is then completely removed from the following analysis.

6 Limits of continuum damage models resp. continuum elastic-plastic models for shell crashworthiness-analyses

The tests by IMRL/ONERA [1], DLR [6] [7] [11], Aerospatiale [2] within the CRASURV project on material coupons show a strong nonlinear behaviour and failure for rather small strains below 0.1%, which is typical for many materials containing Carbon.

For such materials standard continuum material models (see CADFEM [3] [12]) can be applied in a straightforward manner. As long as also **tensile failure** or in many cases **pure shear failure** is concerned, these models might well be applied for crashworthiness situations. However, care has to be taken to avoid mesh dependencies. This is possible, as no further information about the behaviour in the failed region is needed in the simulation.

The situation is **completely different** for problems with **failure in compression**. Then the material behaviour after failure has considerable influence on the total behaviour of a structure. In particular, as strain levels are observed, which may be in the

range of 50 to almost 100%. The visual observation of the failure process in experiments clearly indicates that then a continuum no longer exists; the material structure is deteriorated into single small parts, fibers might still keep some parts together in a rather loose fashion. We have a fragmented material with almost no correlation to the original sheet type orientation, thus a 3D-type behaviour concerning contact among the fragmented material parts must be considered.

However, the tests performed give no indication how such a material law including this phase transition from 2D to 3D may look alike. In particular, there is no information for strains between 0.5 and 50% in compression, which are vital for crashworthiness analyses. All data used for any simulation in this regime are up to now simply taken to fit one or the other structural test. Thus the use of composite material models, which are currently proposed and which are valid for strains up to 1% to 3%, in the large strain compression regime is not based on a solid foundation and cannot be extended for any general simulation.

The solutions using the anisotropic materials within the FE-models also assume that the anisotropy/orthotropy directions are somehow fixed. This is certainly not the case when the fiber angles change during the deformation, as e.g. in Aramid fabric coupon under 45° loading. Then failure surfaces resp. yield functions should take this behaviour into account. However, a complete test series must then be performed to get a basis for further material model developments.

Shell theory for composite laminates at failure?

Classical shell theory is based on the assumption of a linear strain distribution of the strains in membrane direction. In addition the stresses in thickness direction are assumed to be zero. These theories are the basis for the currently most used elements - so-called Reissner-Mindlin elements, single director elements - in the commercial FE programs. For composite laminates the linear strain distribution is certainly a strong restriction, thus more recent theories based on multiple directors e.g. assuming one director for each lamina have been proposed. Then the limits of single director theories concerning improper representation of the shear between the laminas are cured.

Failure representation
Failure in composite laminates under crash loading is dominated by interlaminar shear failure and delamination. For a proper representation of the shear stresses a multidirector theory is essential; for delamination criteria the normal stress in thickness direction of the shell is needed. The standard shell elements do not contain both, thus the failure representation is extremely limited and some artificial adjustments of parameters have to be made to provide a vehicle for these defects.

Comments to lay-ups
If the standard shell theory is used, many of the effects mentioned above seem to be not important and the simulations of composite shell structures often appear to be successful. This is the case, if e.g. single ply failure due to one or more of the above criteria is obtained, and if the laminate as a whole does not show softening and as a consequence no localization in any direction. In fairly complex situation such softening type behaviour resp. localization is hard to detect, as the structure is then often considerably deformed and simple visual checking does not give proper information. The only correct procedure would be to refine the meshes and rerun the analysis and repeat this procedure. However, such an objective approach is scarcely undertaken either due

to time limitations, and as often additional parameter adjustments may be necessary.

7 Summary and Conclusions

In this presentation the composite material models in LS-DYNA, enhanced respectively implemented within the CRASURV project have been described and their failure parameters have been discussed. Using simple test problems, the general mode of operation was shown.

To investigate the composite behaviour, one element tests were performed using not only one anisotropic layer through the thickness to model the composite laminate, but also by considering layers, defining the thickness and the direction of anisotropy of each layer. As a result, the failure of each layer can be investigated, the global behaviour however should remain unchanged. Performing large scale structural analyses, this quantity of information can hardly be handled and therefore it may be preferable to model the complete lay-up only by one single anisotropic layer. Another reason to do so is, that mostly the measured material constants are available only for the composite lay-up as a whole.

Structural simulations – not presented in this contribution – were performed for some structures with simple geometries such as a 90° profile structure and a cylinder, for which experimental data were available. The simulations have shown, that realistic results can be achieved, at least using the crashfront model. However, the set of parameters found to fit the analysis to the experiments is *not* valid for the investigated material in general, but only in combination with a characteristic element size and the considered particular geometry. In addition to this very heuristic crashfront model, the structural behaviour can be influenced by the failure parameters, e.g. it can be made membrane dominated or alternatively bending can be introduced by allowing higher strains before failure.

The main problem however in the simulations was the trigger mechanism to introduce a controlled crushing process. It must be ensured in the simulation model, that no structural failure with element deletion occurs somewhere in the structure, as then an edge-to-edge contact algorithm would be necessary, introducing an extreme complexity into the simulation. Taking the limitations described above into account, realistic simulations can be achieved to some extent; the results, however, must be reviewed very critically before any conclusions from the simulation results can be drawn.

Finally it must be stated, that many measured material data cover only a range of strains up to 0.1 – 1%, in particular for the compressive regime. Crashworthiness involves strains, in particular compressive strains, well above these measured data. In addition, the observation from the experiments indicate that the material deteriorates from a continuum into fragmented parts. Thus any analysis assuming a 2D continuum model – such as in shell analysis – have almost no reasoning for this regime.

As a conclusion it can be said, that the crashworthiness analysis for composite structures has to be carried out with great care. In particular, the regime of applications has to be kept into the limits of continuum mechanics. In general, analyses involving large strains cannot be performed unless further assumptions are taken into account.

References

[1] Deletombe, E.; Delsart, D.: *Commercial aircraft design for crash survivability*, Report No. 97/70 ONERA/IMF Lille (1997).

[2] Thevenet, P.: *Materials testing and generation of a material database*, Aerospatiale Document No. CRASURV-D 1.2.1.1-AS (Nov. 1997).

[3] Hallquist, J.O. *et. al*: *Theory manual*, LSTC report 1018 Rev. 2, Livermore Software Technology Corporation, Livermore, California (1993).

[4] Hallquist, J.O. *et. al*: *Users manual Version 936*, LSTC report 1082, Livermore Software Technology Corporation, Livermore, California (1997).

[5] Kehrt, S.: *Materialprüfung an glasgewebeverstärktem Polyamid (GF-G/PA6.6)*, Internal report, IVW, University of Kaiserslautern (1997) (in German).

[6] Kohlgrüber, D.: *Initial materials data of carbon and aramid fabric materials*, DLR Report within CRASURV DLR-IB 435-97-24 (1997).

[7] Kohlgrüber, D.: *Final materials data of carbon and aramid fabric materials*, DLR Report within CRASURV DLR-IB 435-98-23 (1998).

[8] Johnson, A.F.; Kindervater, C.M.: *Review of crashworthiness research on composite structures*, DLR Report within CRASURV DLR-IB 435-97/21 (1997).

[9] Matzenmiller, A.; Lubliner, J.; Taylor, R.L.: *A constitutive model for anisotropic damage in fiber-composites*, Mechanics of Materials **20** pp. 125-152 (1995).

[10] Michielsen, A.L.P.J.; Wiggenraad, J.F.M.: *Review of crashworthiness research of composite structures*, Technical Report NLR CR 97046 L, Nationaal Lucht- en Ruimtevaartlaboratorium, Netherlands (1997).

[11] Schon, U.: *FE-Simulation des Crashverhaltens von einfachen Probekörpern aus Faserverbundwerkstoff mit begleitendem experimentellen Bezug*, Studienarbeit am Institut für Flugzeugbau, University of Stuttgart (1996) (in German).

[12] Schweizerhof, K.; Maier, M.; Matzenmiller, A.; Rust, W.: *Composite crash elements for energy absorption in frontal crash situations*, VDI Berichte 1007, VDI-Verlag Düsseldorf, pp. 523-546 (1992).

[13] Schweizerhof, K.; Muenz, T.; Weimar, K.; Rottner, T.: *Improving and testing the composite materials in LS-DYNA for crash problems — a critical survey*, Rep.No. CRASURV 2-1, 2/98, EC Project, CADFEM GmbH Grafing (1998).